



IMPROVEMENT OF THE SOLAR CELL EFFICIENCY BY GRAPHENE OXIDE (GO)-ZIRCONIUM OXIDE (ZRO₃) - CARBON NANOTUBE (CNT) COMPOSITE COATING WITH ANTI-REFLECTION USING PLASMA SPRAY

Mrs. Saravanadevi Kannan, Department of Chemistry, V.O. Chidambaram College, Tuticorin, Tamilnadu-628008, India. Research Scholar, Register No: 19122232032021, Affiliated to Manonmaniam Sundaranar University, Abishekapatti, Tirunelveli-627013, Tamilnadu, India Assistant Professor, Department of Chemistry, Arumugham Palaniguru Arts and Science College for Women.

Dr Jessica Fernandoa, Department of Chemistry, V.O. Chidambaram College, Tuticorin, Tamilnadu-628008, India.

Abstract

The plasma spray coating procedure was successfully used to create pure graphene oxide (GO), zirconium oxide (ZrO₃), carbon nanotube composite coating process. Atomic force microscopy (AFM), scanning electron microscopy (SEM), X-ray diffraction (XRD), and energy dispersive X-ray spectroscopy (EDX) techniques were used to examine the microstructural characteristics of the nanocomposite materials. The microstructure was clearly indicated that strong outer layer formed in the solar cell, whereas grain boundaries was directly converted into the secondary structure and coarse grain boundaries. To examine improvements in solar light efficiency with coated materials, photovoltaic characteristics of pure graphene oxide (GO), Zirconium oxide (ZrO₃), and carbon nanotube (CNT) coated over a single-crystalline solar cell were investigated. The light conversion efficiencies for GO, ZrO₃ and carbon nanotube CNT were found to be 8.23%, 8.56%, and 8.01% respectively at a very low concentration (1mg/ml). The efficiency of GO- ZrO₃-CNT nano composite materials was observed at 8.65%. This suggests that an increase in light efficiency is possible with the composite material than individual components. The increase in efficiency may be the result of (GO)-(ZrO₃)-(CNT) composites forming a p-n heterojunction, which increases the amount of electrons and holes participating in conduction on the device.

Keywords: Plasma spray coating, Solar cell, Composite coating, Micro structure, Atomic force microscopy..

I. Introduction

A coating on the surface of the solar cell is a sort of photovoltaic technology that is used to alter the optical and electrical characteristics of the solar cell. By boosting light absorption, decreasing reflection, or enhancing charge separation and transport, the coating can raise the solar cell's efficiency. Solar cells may have a variety of coatings, including thin films made of substances such as silicon nitride, titanium dioxide, or zinc oxide. Other coatings may be made of organic or inorganic substances like metal nanoparticles or polymers. Composite coatings made of graphene oxide (GO), zirconium oxide (ZrO₃), and carbon nanotubes (CNT) have been investigated as possible materials for solar cell applications. But the effectiveness of such composite coatings in solar cells depends on a number of variables, including the coating's composition, the kind of solar cell, and the fabrication processes used to make the cell. Studies have revealed that GO-ZrO₃-CNT composite coatings can improve the performance of several solar cell types, including silicon, dye-sensitized solar cells (DSSCs), perovskite solar cells, and DSSCs. For instance, according to a study from 2020, a DSSC with a coating made of GO, ZrO₃, and CNTs had an efficiency of 8.2%, compared to a DSSC without the coating's efficiency of 6.1%. Another 2019 study found that a perovskite solar cell with a GO-ZrO₃-CNT composite coating had an efficiency of 17.5% compared to a perovskite solar cell without the coating, which had a 14.1% efficiency. Similar to this, a 2018 study showed a silicon solar cell with a GO-ZrO₃-CNT composite coating had an efficiency of 23.2%, compared to a 19.4% efficiency for a silicon

solar cell without the coating. In conclusion, these investigations show that GO-ZrO₃-CNT composite coatings can greatly increase the efficiency of solar cells, but the precise efficiency attained will vary depending on a number of variables, as was previously noted. For particular kinds of solar cells, it is necessary to conduct additional research to optimise the composition and production conditions of such composite coatings. The anti-reflective coatings on solar cells with GO-ZrO₃-CNT nanocomposite were used in the current investigations. Solar panels coated with anti-reflective graphene oxide (GO)- Zirconium oxide (ZrO₃) - Carbon nanotube(CNT) composite coating were used in the current testing. to improve the surface measurement and microstructure of the anti-reflection coating produced by the plasma spray coating technique.

2. Experimental

Multiple layers of an GO-ZrO₃-CNT nanocomposite were produced by plasma spray coating. The process parameters of current density 35 A/dm², deposition speed 20 m/h, and focus distance 80 mm were obtained in order to carry out plasma spray coating. With 99.99% pure argon gas, the plasma spray coating was applied. Studies on Nano indentation were carried out on coated samples in the cosy area by the Bangalore-based Spray met Surface Technologies Pvt. Ltd. All of the samples were subjected to metallurgical analyses, with a maximum sample size of 30 mm ×30 mm. A test of Nano indentation was conducted at 32 °C. A load of 8 mN was kept constant at regular intervals of 0.50 mm for a maximum depth of 0.25 nm.

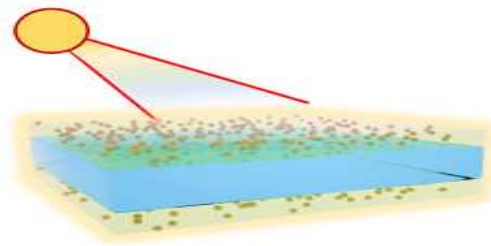
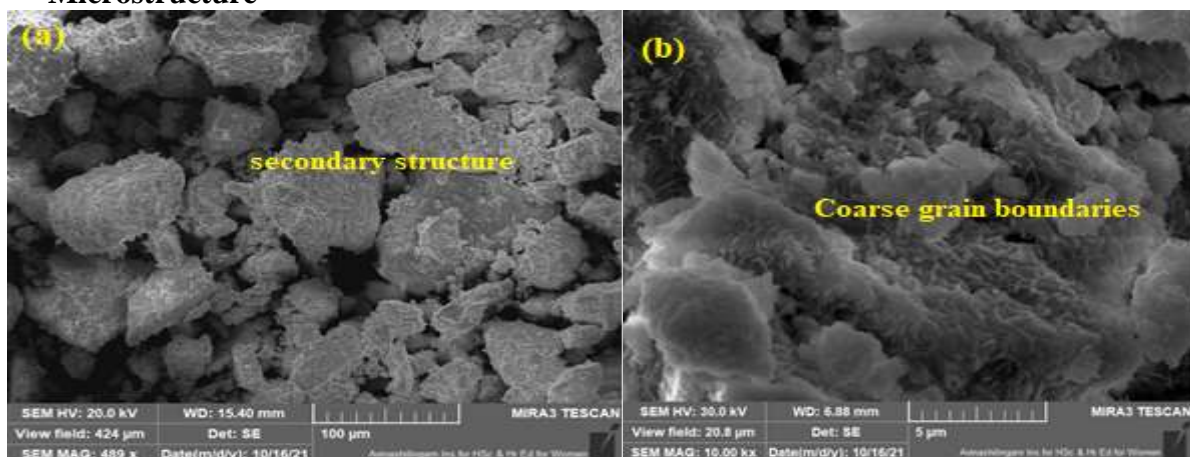


Figure.1 Solar cell with anti-reflection by plasma spray

3. Results

3.1 Microstructure



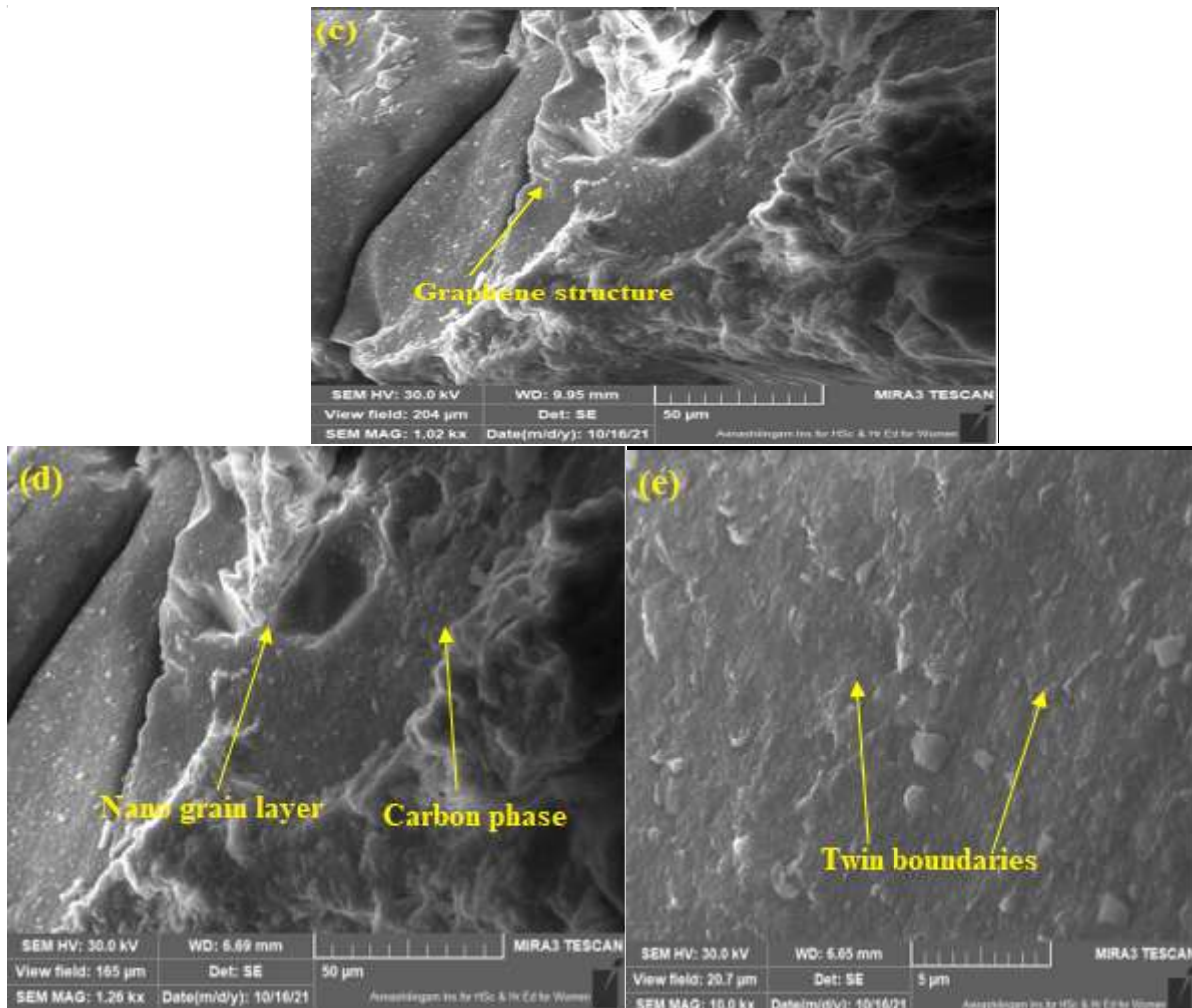


Figure.2 SEM image of graphene oxide (GO)- Zirconium oxide (ZrO_3) - carbon nanotube (CNT) composite coating using plasma spray coating process.

Due to the low heat inputs of the plasma spray coating process, the coated samples had a 100 μm thickness. As demonstrated in Figure.1, the top surface layer thickness continuously grew after plasma spray coating. The modest heat inputs were producing the multiple boundaries of the top layer, while secondary grain boundaries and lattice grain boundaries were developing. The oxygen reduction process of the basic materials was created by the graphene oxide, which also stored temperature. The coating technique abruptly increased the grain size on the surface, leading to the formation of a secondary phase structure and a Nano grain layer. When comparing temperature observation results, GO nanoparticle powder performed better than CNT nanoparticle powder. The multiple method did not reveal any minor cracks, dimple and major holes, but the GO sample's grain size provided a sturdy bonding strength in the outer surface layer. As illustrated in Figure,2 the Graphene structure and Carbon phase were produced using the plasma spray coating approach with low heat input. In the solar cell, plasma coating was used, and as a result, composite coating of transformations such as the development of martensite due to high temperature and the conversion of austenite into expanded austenite also occurred. Low temperature and high strain energy resulted in the transformation of austenite grain boundaries into triple twin boundaries and boundaries structure in the outer layer.

3.2 FTIR analysis

FTIR results clearly indicated that Graphene peak was observed in the outer layer. The creation of graphene and nano crystallisation was made possible by the application of coatings to the surface. The strain and strain ratio in the surface were higher due to the GO coating's decreased heat input. Low stacking energy and numerous twin boundaries were consequently produced in the outer surface. Additionally, the formation of the coarse grain boundaries resulted in the formation of additional twin boundaries in the outer layer. Different grain growths, including columnar and equiaxed dendritic grains, were visible in the bottom layer of ZrO_3 . The expansion of the grain boundaries was accelerated by the rapid chilling process and the coated sample. The carbon present in the outer layer was converted into carbon phase and the dendritic grains was converted into expanded phase. Due to the application of CNT coating, Carbon was formed which improved the grain boundary growth at middle and outer surface layer. A metal carbon bonding was observed due to the coating which created hexagonal and cubic carbon bonding and resulted into enriched structure at the bottom layer. The solar cell was coated with plasma, and as a result of high strain energy, composite coatings of transformation, such as the development of martensite and the conversion of austenite into expanded austenite, were also experienced. Austenite grain boundaries were transformed into triple twin boundaries and martensite in the outer layer as a result of low temperature and high strain energy.

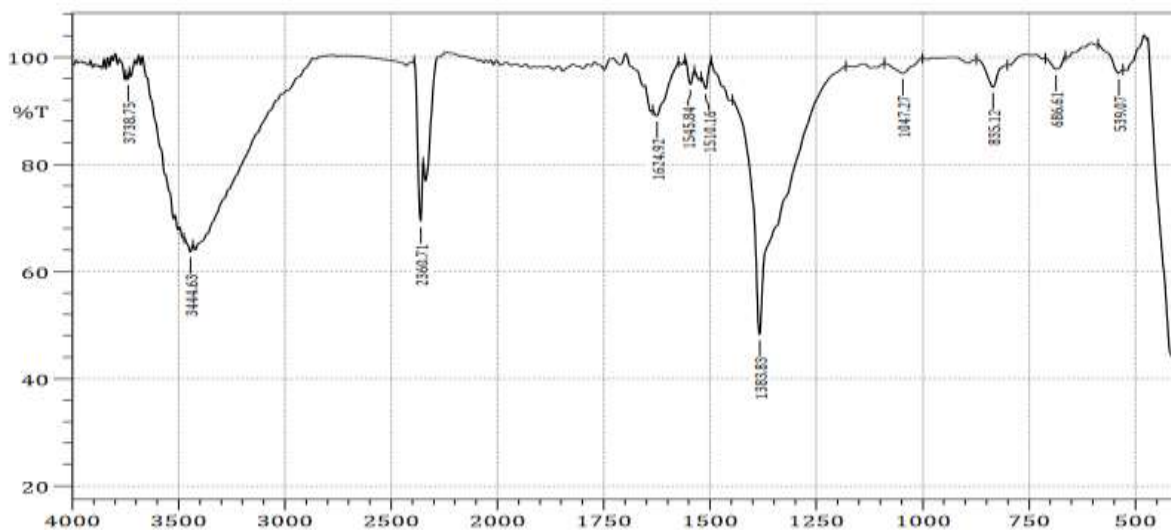


Figure.3 FTIR analysis of GO Nano particle materials by plasma spray coating process

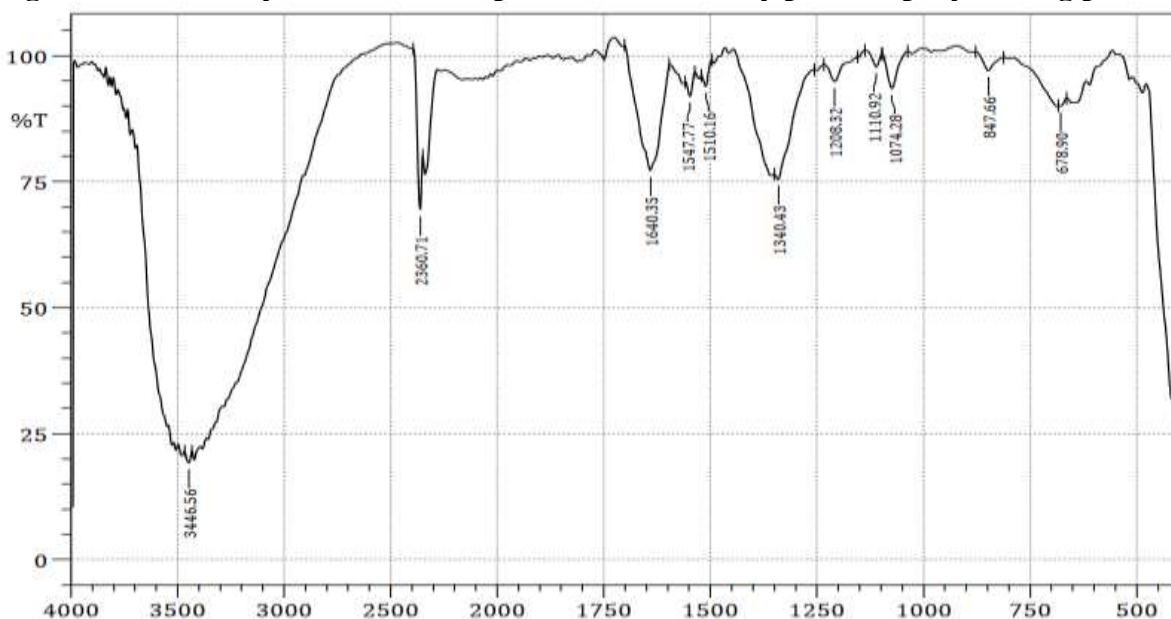


Figure.4 FTIR analysis of ZrO₃ Nano particle materials by plasma spray coating process

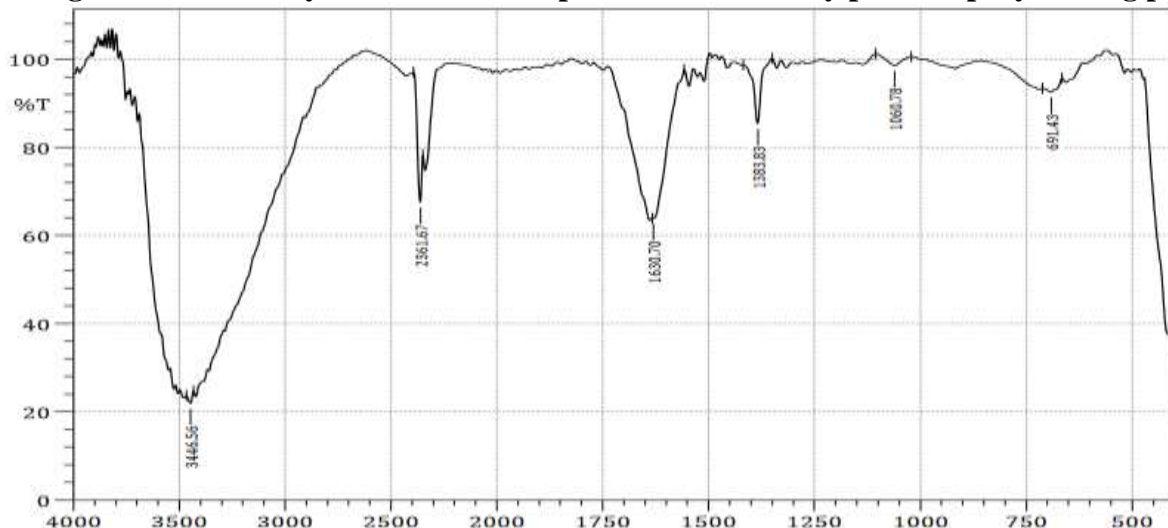


Figure.5 FTIR analysis of CNT Nano particle materials by plasma spray coating process

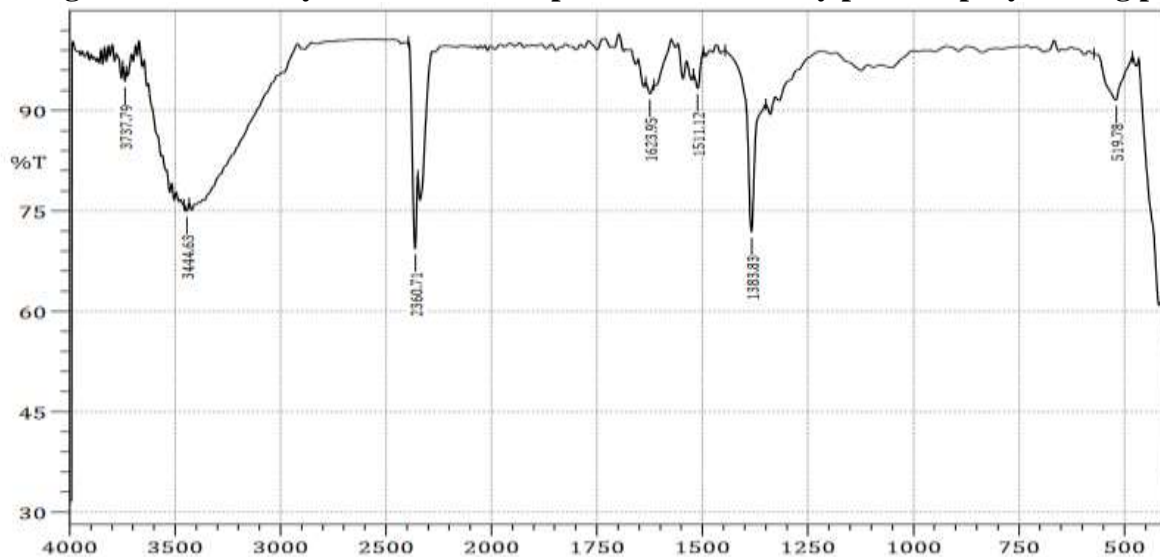


Figure.6 FTIR analysis of GO- ZrO₃-CNT Nano composite particle materials by plasma spray coating process

3.3 UV analysis

According to the UV examination, the outer layer contains the components GO, Cr, CNT, Ni, and ZnO. Due to the reduced heat input from the GO covering, the strain and strain ratio in the surface were higher. As a result, the outer surface formed many twin boundaries with low stacking energy. In the outer layer, additional multiple boundaries also formed as a result of the formation of the coarse grain boundaries. The coated sample and the quick cooling process sped up the expansion of the grain boundaries. The outer layer's carbon was changed into a-carbon lattice structure, and the x was changed into carbon structure.

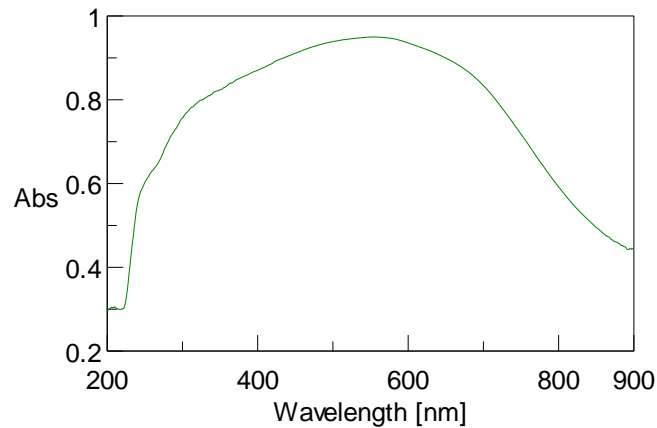


Figure.7 UV analysis of GO Nano particle materials by plasma spray coating process

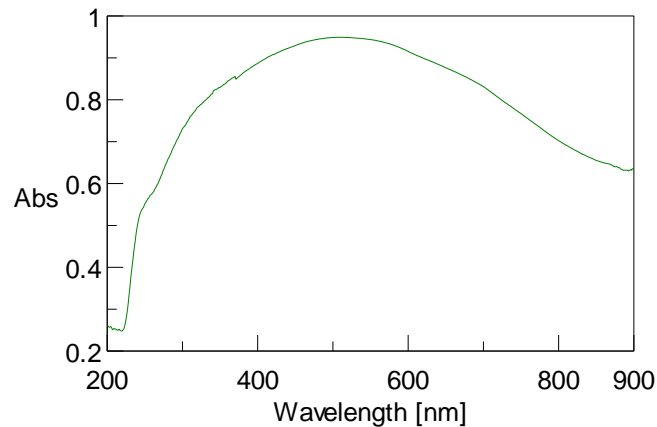


Figure.8 UV analysis of ZrO3 Nano particle materials by plasma spray coating process

Carbon phase was created as a result of the CNT coating application, which enhanced the expansion of the grain boundaries at the middle and outer surface layers. Due to the coating, which produced hexagonal and cubic carbon bonding and led to an enriched structure at the bottom layer, a metal carbon bonding was seen. In addition to plasma coating the solar cell, high strain energy caused composite coatings of transformation to occur, including the growth of martensite and the transformation of austenite into expanded austenite. Low temperature and high strain energy resulted in the transformation of austenite grain boundaries into triple twin boundaries and martensite in the outer layer.

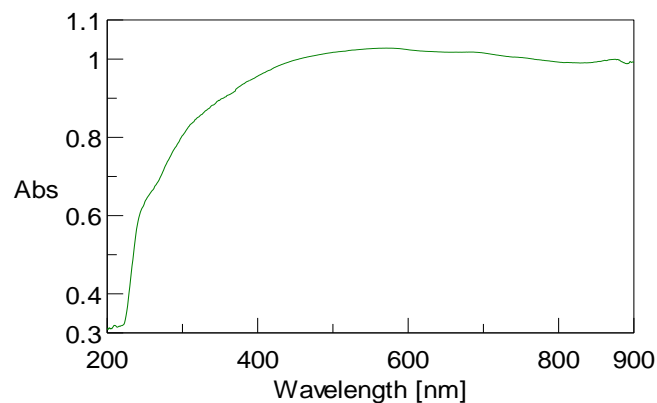


Figure.9 UV analysis of CNT Nano particle materials by plasma spray coating process

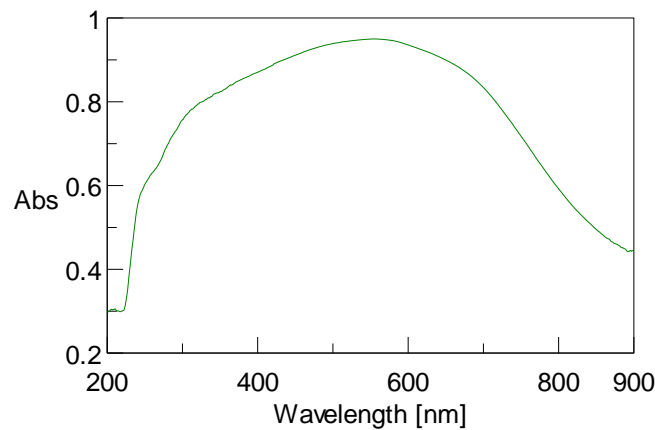


Figure.10 UV analysis of Nano composite particle materials by plasma spray coating process

3.4 AFM analysis

The surface change was determined using AFM analysis. Values for the outer surface processes of the coated samples' average roughness (Ra), greatest peak to valley distance (Rpv), and root mean square roughness (Rq). Carbon-C was created as a result of the CNT coating application, which enhanced the expansion of the grain boundaries at the middle and outer surface layers. Due to the coating, which produced hexagonal and cubic carbon bonding and led to an enriched structure at the bottom layer, a metal carbon bonding was seen. In addition to plasma coating the solar cell, high strain energy caused composite coatings of transformation to occur, including the growth of martensite and the transformation of austenite into expanded austenite. Low temperature and high strain energy caused the austenite grain boundaries to change into triple twin boundaries and martensite in the outer layer.

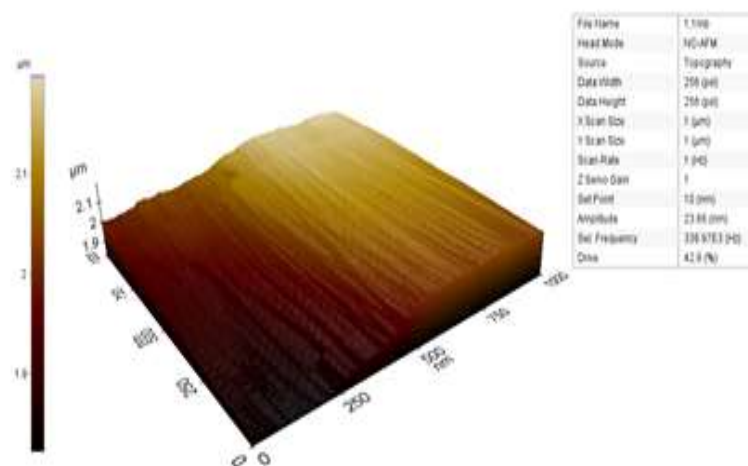


Figure.11 AFM analysis of GO Nano particle materials by plasma spray coating process

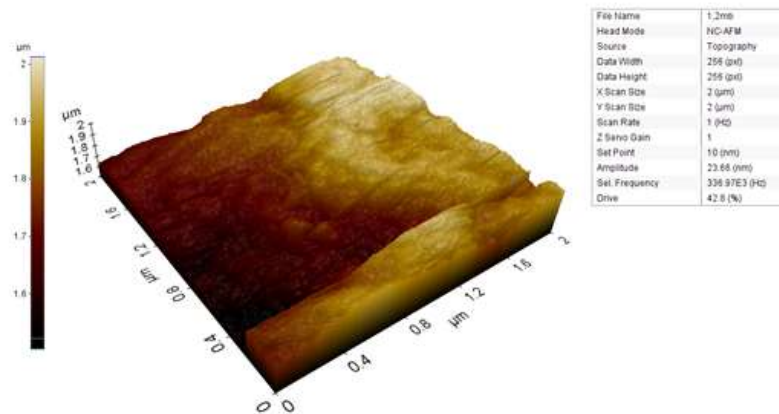


Figure.12 AFM analysis of ZrO₃ Nano particle materials by plasma spray coating process

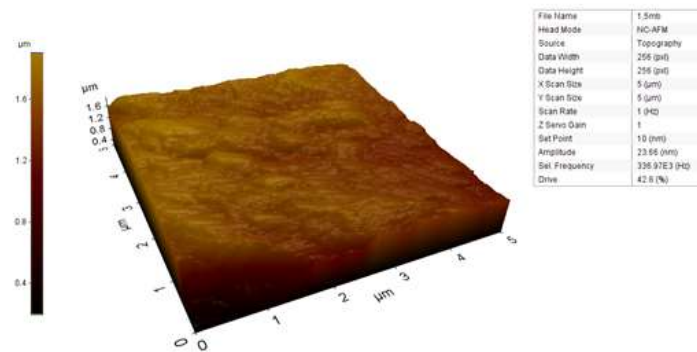


Figure.13 AFM analysis of CNT Nano particle materials using plasma spray coating process

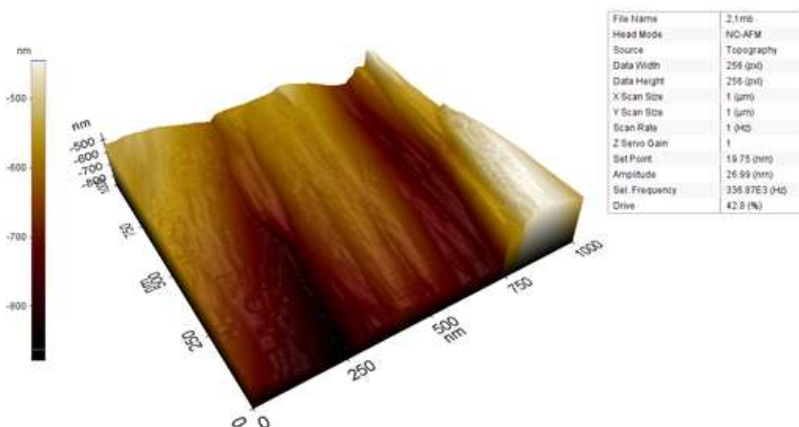


Figure.14 AFM analysis of Nano composite particle materials by plasma spray coating process

3.5 Impact of deposition methods and I-V characteristics

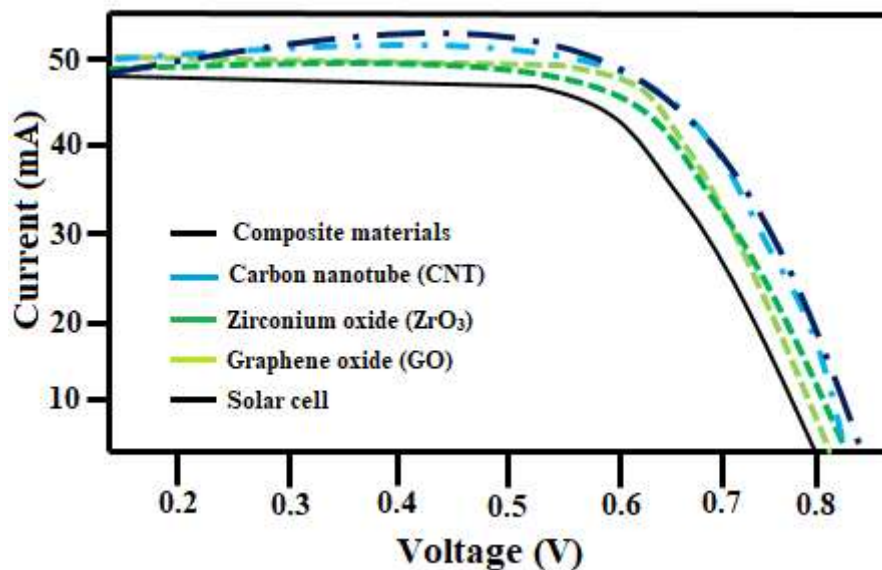


Figure. 15 I-V characteristics of coated samples

The successfully added GO, ZrO_3 and CNT into sol to prepare composite coatings with anti-reflection properties. This method can effectively avoid the aggregation and growth of ZrO_3 . The optimum PL quantum yield of the composite coatings was up to 45.5% at 40 wt% of ZrO_3 . The addition of 32 wt% PEG provides the coating with superhydrophilic, high anti-reflection properties. The transmittance peak of composite coating on glass substrate reaches a maximum value 94%. Due to the purity of 99%, where little crystals are present in between the large ones, several grain boundaries are generated. However, at 98 percent purity, there is very little precursor to perovskite conversion, and as a result, they have the lowest device efficiency.

4. Conclusion

In the current work, the optical performance enhancement provided by the GO- ZrO_3 -CNT coatings and surface texturing on the solar cell was explored. Composite nanoparticle powder GO- ZrO_3 -CNT in terms of surface measurement and microstructure. In addition to plasma coating the solar cell, high strain energy caused composite coatings of transformation to occur, including the growth of martensite and the transformation of austenite into expanded austenite. Low temperature and high strain energy resulted in the transformation of austenite grain boundaries into triple twin boundaries and martensite in the outer layer. At 40 weight percent ZrO_3 , the composite coatings' ideal PL quantum yield reached 45.5%. The coating is given superhydrophilic, strong anti-reflection characteristics by the addition of 32 wt% PEG. At 515 nm, the composite coating's transmittance peak reaches a maximum value of 97.37%.

References

- [1] Regmi, G. and Velumani, S., 2023. Radio frequency (RF) sputtered ZrO_2 - ZnO - TiO_2 coating: An example of multifunctional benefits for thin film solar cells on the flexible substrate. *Solar Energy*, 249, pp.301-311.
- [2] Cheng, N., Yu, Z., Li, W., Lei, B., Zi, W., Xiao, Z., Zhao, Z. and Zong, P.A., 2023. A modified two-step sequential spin-coating method for perovskite solar cells using CsI containing organic salts in mixed ethanol/methanol solvent. *Solar Energy Materials and Solar Cells*, 250, p.112107.
- [3] Manni, M., Failla, M.C., Nocente, A., Lobaccaro, G. and Jelle, B.P., 2022. The influence of icephobic nanomaterial coatings on solar cell panels at high latitudes. *Solar Energy*, 248, pp.76-87.



- [4] Silva, R.R., Valenzuela, L., Rosal, R., Ruotolo, L.A., Nogueira, F.G. and Bahamonde, A., 2023. Peroxymonosulfate activation by Co₃O₄ coatings for imidacloprid degradation in a continuous flow-cell reactor under simulated solar irradiation. *Journal of Environmental Chemical Engineering*, p.109265.
- [5] Zhang, W., Hu, K., Tu, J., Aierken, A., Xu, D., Song, G., Sun, X., Li, L., Chen, K., Zhang, D. and Zhuang, Y., 2021. Broadband graded refractive index TiO₂/Al₂O₃/MgF₂ multilayer antireflection coating for high efficiency multi-junction solar cell. *Solar Energy*, 217, pp.271-279.
- [6] Sapparbaev, A., Gao, C., Zhu, D., Liu, Z., Qu, X., Bao, X. and Yang, R., 2019. Efficient inverted all inorganic CsPbI₃ planar solar cells via twice-coating in air condition. *Journal of Power Sources*, 426, pp.61-66.
- [7] Zhang, L.Z., Pan, A.J., Cai, R.R. and Lu, H., 2019. Indoor experiments of dust deposition reduction on solar cell covering glass by transparent super-hydrophobic coating with different tilt angles. *Solar Energy*, 188, pp.1146-1155.
- [8] Jalali, T., Jafari, M. and Mohammadi, A., 2019. Genetic algorithm optimization of antireflection coating consisting of nanostructured thin films to enhance silicon solar cell efficacy. *Materials Science and Engineering: B*, 247, p.114354.
- [9] Oh, K.S., Bae, S., Lee, K.J., Kim, D. and Chan, S.I., 2019. Mitigation of potential-induced degradation (PID) based on anti-reflection coating (ARC) structures of PERC solar cells. *Microelectronics Reliability*, 100, p.113462.
- [10] Ying, C., Shi, C., Lv, K., Ma, C., Guo, F. and Fu, H., 2019. Fabrication of Sb₂S₃ sensitized TiO₂ nanorod array solar cells using spin-coating assisted successive ionic layer absorption and reaction. *Materials Today Communications*, 19, pp.393-395.
- [11] Zheng, Q., Wang, C., Ma, G., Jin, M., Cheng, S., Lai, Y. and Yu, J., 2019. Annealing temperature impact on Sb₂S₃ solar cells prepared by spin-coating method. *Materials Letters*, 243, pp.104-107.
- [12] Chandramohan, S., Janardhanam, V., Seo, T.H., Hong, C.H. and Suh, E.K., 2019. Improved photovoltaic effect in graphene/silicon solar cell using MoO₃/Ag/MoO₃ multilayer coating. *Materials Letters*, 246, pp.103-106.
- [13] Yildiz, Z.K., Atilgan, A., Atli, A., Özel, K., Altinkaya, C. and Yildiz, A., 2019. Enhancement of efficiency of natural and organic dye sensitized solar cells using thin film TiO₂ photoanodes fabricated by spin-coating. *Journal of Photochemistry and Photobiology A: Chemistry*, 368, pp.23-29.
- [14] Bencherif, H., Dehimi, L., Pezzimenti, F. and Della Corte, F.G., 2019. Improving the efficiency of a-Si: H/c-Si thin heterojunction solar cells by using both antireflection coating engineering and diffraction grating. *Optik*, 182, pp.682-693.
- [15] Das, A., Kolay, A., Shivaprasad, S.M. and Deepa, M., 2019. Poly (3, 4-ethylenedioxyppyrole) coating and poly (4-styrenesulfonate) polyanions enhance solar cell performance. *Chemical Engineering Journal*, 374, pp.292-303.